Talanta 83 (2010) 482–492

Contents lists available at ScienceDirect

Talanta

journal homepage: www.elsevier.com/locate/talanta

Development of membrane inlet mass spectrometry for examination of fermentation processes

Juan-Rodrigo Bastidas-Oyanedel[a], Zuhaida Mohd-Zaki[b], Steven Pratt[b], Jean-Philippe Steyer[a], Damien J. Batstone[b,*]

[a] INRA, UR0050, Laboratoire de Biotechnologie de l'Environnement, Avenue des Etangs, Narbonne F-11100, France
[b] Advanced Water Management Centre (AWMC), Environmental Biotechnology CRC, The University of Queensland, St Lucia, Brisbane, QLD 4072, Australia

ARTICLE INFO

Article history:
Received 29 April 2010
Received in revised form 2 September 2010
Accepted 25 September 2010
Available online 1 October 2010

Keywords:
Membrane inlet mass spectrometry
Calibration
Anaerobic fermentation
Hydrogen
Carbon dioxide
Ethanol

ABSTRACT

Membrane inlet mass spectrometry (MIMS) is useful for on-line monitoring of fermentation processes. However, readings are affected by the complex and dynamic matrix in which biological processes occur, making MIMS calibration a challenge. In this work, two calibration strategies were evaluated for measurement of typical products of acidogenic fermentation, i.e., ethanol, H_2, and CO_2 in the liquid phase, and H_2 and CO_2 in the gas phase: (1) "standard calibration", which was performed independent of fermentation experiments with sterile standards in water with a N_2 headspace, and (2) "in-process calibration" whereby fermentation was monitored concurrent with off-line analysis. Fermentation was operated in batch and continuous modes. In-process calibration was shown to be most effective for measurements of H_2 and CO_2 in both gas and liquid phases; standard calibration gave erroneous results. In the gas phase, this was due to a lower sensitivity during experiments compared to the independent standard calibration, believed to be caused by formation of a liquid film on the surface of the probe. In the liquid phase, moving from the standard calibration environment to the fermentation caused the linear relationship between the H_2 concentration and MIMS signal to change in intercept, and the relationship for CO_2 to change in slope, possibly due to dissolved ions, and related non-ideality. For ethanol, standard calibration results were fairly consistent with in-process calibration results. The main limitation with in-process calibration is the potential for a lack of variability in target concentration. This could be addressed by spiking the targeted compound at the end of the experiment. Regardless, MIMS is an ideal instrument for analysing fermentation experiments, due to its ability to measure targeted compounds semi-continuously, and due to a lack of drift over long periods.

1. Introduction

Membrane inlet mass spectrometry (or membrane introduction mass spectrometry, MIMS) is a method of introducing analytes into a mass spectrometer's vacuum chamber via a semipermeable membrane [1]. MIMS is most useful for the measurement of small, non-polar molecules, since they have a high affinity to the membrane. After samples have been extracted via the membrane, they are analysed by a mass spectrometer. A more detailed description is given elsewhere [2]. Membrane inlet mass spectrometry has the following advantages over other on-line analytical methods: (1) minimally invasive technique, (2) rapid response of seconds to minutes, (3) measures volatile compounds up to 200 molecular weight, (4) high sample frequency, (5) high sensitivity (e.g., 0.25 μM O_2), (6) measurements can be made in gas and/or liquid phase, and (7) low analytical costs [3]. Disadvantages include preferential retention of some compounds (e.g., H_2S) causing memory effects [4], however, the major issue is that the MIMS signal is not a direct measure of target concentration, but rather a measure of the ionization of compounds that pass through the membrane [5]. Calibration is therefore crucial in order to have an absolute measure of the analyte.

MIMS signal magnitude not only depends on the volatility of the analyte, but also depends on sample and experimental conditions, including membrane permeability, temperature, ionization, sample point hydraulics, and sample matrix composition [5]. These issues need to be addressed during calibration of the signal. With good control of experimental equipment, the most variable of these is chemical matrix. Chemical components can influence permeation rates and ionization efficiencies of analytes, cause long-term memory effects and change membrane properties [6,7]. There is generally limited calibration information available, and early work

* Corresponding author. Fax: +61 7 3365 4726.
E-mail addresses: oyanede@supagro.inra.fr, yanauta@gmail.com (J.-R. Bastidas-Oyanedel), z.zaki@uq.edu.au (Z. Mohd-Zaki), s.pratt@awmc.uq.edu.au (S. Pratt), steyer@supagro.inra.fr (J.-P. Steyer), damienb@awmc.uq.edu.au (D.J. Batstone).

0039-9140/$ – see front matter © 2010 Elsevier B.V. All rights reserved.
doi:10.1016/j.talanta.2010.09.034

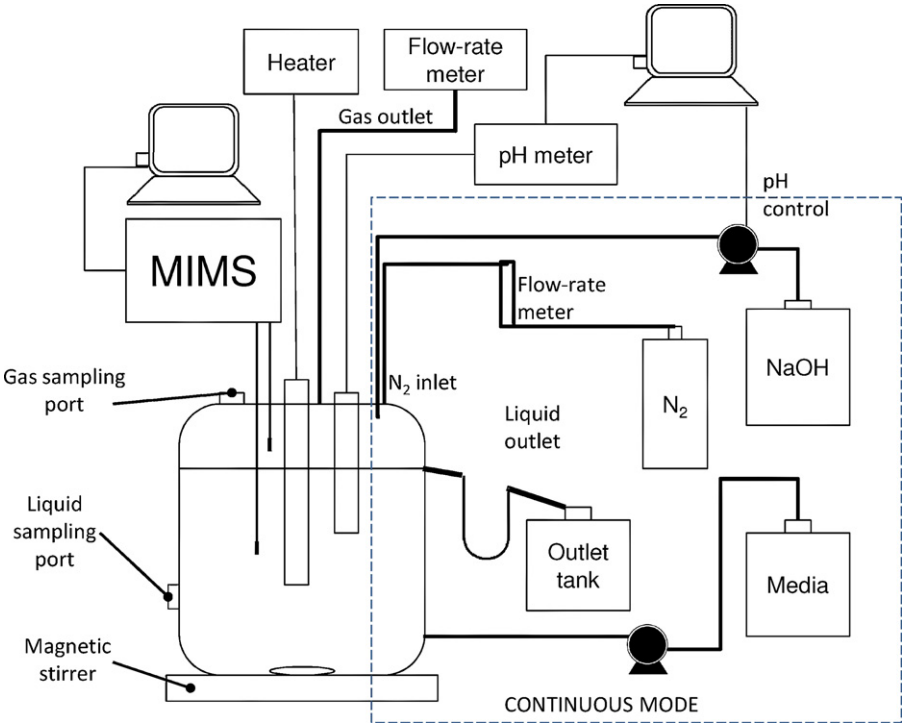

Fig. 1. Reactor diagram. Modules surrounded by the dashed square were added to the rest of the equipments at the continuous fermentation mode.

using MIMS did not calibrate against an external reference, but instead presented relative kinetics [8,9]. Hillman et al. [10] and Radivojevic et al. [11] translated MIMS signals by estimating dissolved concentrations of gases in water using gas partial pressures and Henry law. Standard solutions [3,12–17] have been used, but this results in a different matrix from the sample. Heinzle and Lafferty [6] showed that three different liquid solutions (pure water, normal nutrient solution and sterilized fermentation broth) have an impact on calibration curves for dissolved H_2 and O_2. They also showed that presence of viable cells had an impact, and concluded that standard solution calibration was not suitable for biochemical experiments. Andersen et al. [18] attempted to address matrix issues by resuspending a known amount of viable cells into the calibration solutions. Yang et al. [4,19] used corrections in CO_2 MIMS signal for pH and ionic strength. Lloyd and James [20] used standard additions in fermentation experiments at constant pH and temperature. This approach was followed by other workers [21,22]. This is effective and is one approach to in-process calibration, but it has a chemical impact on the underlying processes. This approach also does not effectively address solutions' non-ideality. In addition, standard additions require a compound that is relatively easy to add, which is not the case for dissolved gases.

The best way to address variability in chemical matrix and other conditions is by off-line measurement against a matrix-independent method. This was done by Doerner et al. [23] and Tarkiainen et al. [7] who determined that calibration against standards was unsuccessful. They examined how different mixtures of gases and volatiles affect membrane transfer properties, and consequently MIMS signal magnitude. The conclusion was that MIMS signal calibration for fermentation processes has to be based on conventional off-line analysis such as gas chromatography.

Hence, calibration based on off-line analysis seems to be an effective method, but there is a lack of detailed information, particularly for measurement of dissolved gases in the liquid phase. This is critical for H_2 and CO_2 that are major products of acidogenic fermentation. H_2 is increasingly being investigated as a renewable fuel. The issues around H_2 are complicated by high diffusivity, low solubility, and a high degree of non-ideality in relation to the matrix. While dissolved CO_2 concentration is highly affected by liquid matrix pH. The purpose of this study is thus to assess MIMS calibration methods for fermentation experiment systematically, and particularly with respect to dissolved gases.

2. Materials and methods

2.1. Fermentation experiments

Fermentation and calibration procedures were performed in a mixed culture fermentation system, using a glass reactor, with constant temperature, headspace pressure (regulated through a gas flow-rate meter), liquid stirring velocity, gas and liquid volumes. Feed was glucose in basal anaerobic (BA) media. Two different fermentation modes were performed; continuous and batch. During continuous experiments, the system was operated at a constant feed rate, with optional flushing of the headspace with N_2 to change gas partial pressures. During batch experiments, dynamics were assessed by introducing a glucose pulse at time 0.1 days. MIMS probes were used in gas and liquid phases simultaneously.

2.1.1. Reactor equipment

A diagram of the experimental equipment is shown in Fig. 1. Liquid volume was 1.31 L and a headspace of 170 mL. Temperature was regulated at 37 °C using an immersed glass heater (25W Aqua One™). A magnetic stirrer was used at approximately 600 rpm. For continuous experiments, the system was fed by a Watson Marlow peristaltic pump from split feed tanks containing basal media, and pure glucose solution. pH was controlled by a pH probe and peristaltic pump feeding 1 M NaOH. Liquid lock was maintained by a glass U-tube. Gas flow was measured by a tipping-bucket type meter, with a bucket volume of 2 mL, and a constant pressure of approximately 1 cm water. MIMS probes were placed both in gas and liquid phases, respectively. All equipment was interfaced to computers via an Opto PLC used for data logging and set-point mod-

ification. N_2 flushing of the headspace was also available, with pure N_2 flow being regulated through parallel Cole Parker rotameters with limits of 0.5 mL·min^{-1} and 5 mL·min^{-1} (allowing full range of flow regulation).

2.1.2. Media

Feed was held in two containers (in order to avoid microbial contamination), fed simultaneously. Substrate solution consisted of 10 g·L^{-1} of glucose and silicone based antifoam (Dow Corning® antifoam RD emulsion) at 1 mL·L^{-1}, autoclaved at 120 °C for 45 min. The basal anaerobic (BA) media contained in mg·L^{-1}: 2.4 $CaCl_2{\cdot}2H_2O$, 0.1 $(NH_4)_6Mo_7O_{24}{\cdot}4H_2O$, 0.1 $CoCl_2{\cdot}6H_2O$, 4 $FeCl_2{\cdot}4H_2O$, 0.1 $MnCl_2{\cdot}4H_2O$, 0.184 $NiCl_2{\cdot}6H_2O$, 0.2 $Na_2SeO_3{\cdot}5H_2O$, 0.1 H_3BO_3, 0.076 $CuCl_2{\cdot}2H_2O$, 0.1 $ZnCl_2$, 0.1 $AlCl_3$, 1 EDTA, 0.01 aminobenzoic acid, 0.004 biotin, 0.004 folic acid, 0.01 nicotinic acid, 0.01 panthothenic acid, 0.02 pyridoxine, 0.01 riboflavin, 0.01 thiamine hydrochloride, 0.0002 cyanocobalamine, 0.01 lipoic acid; in g·L^{-1}: 2 NH_4Cl, 0.2 NaCl, 0.2 $MgCl_2{\cdot}6H_2O$, 0.2 $K_2HPO_4{\cdot}3H_2O$, and 0.2 $Na_2S{\cdot}9H_2O$; and HCl 2 (μL·L^{-1}). BA media was based on Angelidaki and Sanders [24], modified to minimize calcium phosphate precipitation.

2.1.3. Inoculum

Inoculum was anaerobic digestate from a primary sludge fed digester in Brisbane, Australia. The inoculum was conditioned by operation at 12 h hydraulic retention time (HRT) over 1 week without pH control (native pH of 5.5), until methane production stopped, giving as a result a standardized mixed culture fermentative community.

2.1.4. Batch experiments

Initial conditions were established by continuous mode fermentation over two days, with pH controlled at 6.5, and a HRT of 6 h. Prior to batch experiments, MIMS signal was stable for at least 12 h. Batch experiments consisted of a halt in feed, and injection of 2 mL autoclaved solution containing 325 g·L^{-1} glucose. After 24 h, a new glucose pulse was added to the bioreactor.

2.1.5. Continuous experiments

Continuous mode involved constant feed via a peristaltic pump. In experiments presented here, a pH set-point of 6.5 was used, with a HRT of 6 h. Changes in the gas phase composition were achieved by flushing the headspace with N_2 at 0, 2.5, 7, and 50 L·d^{-1} over a period of 6 days. Flushes indirectly changed liquid partial pressures. Liquid partial pressures were not changed by sparging, as this would also severely change mixing intensity over the MIMS probe.

2.2. MIMS set-up and operation

A commercially available Hiden HPR-40 DSA dissolved species analyser bench top MIMS unit (Hiden Analytical Ltd., Cheshire, England) was used, which contained a Hiden HAL 201 RC quadrupole mass spectrometer with dual faraday/electron multiplier detector and a mass range of 200 atomic mass units. MIMS unit inlets consist of a 4 way multistream selector for simultaneous sampling. Each MIMS probe had 0.5 m length, suited with silicon rubber membrane. Recorded mass to charge (m/z) ratio was 1, 31, and 44 for H_2, ethanol and CO_2, respectively. The m/z ratios were selected after scanning these three pure compounds during previous experiments.

2.3. MIMS signal translation

The different experiments were used to identify the different impacts of experimental equipment (including hydraulics), and sample chemical matrix on MIMS signal translation into quantitative information, i.e., composition of targeted compounds in gas and/or liquid phase.

2.3.1. Standard calibration

In this procedure, standard matrix consisted on reversed osmosis (RO) water liquid phase and N_2 gas phase. Temperature and agitation were the same as in both batch and continuous fermentations. Pure compounds were added at different ratios into the reactor in order to cover their expected concentration range during fermentation. Pure H_2 was injected into the headspace reactor to give the following H_2 partial pressures: 0, 0.2, 0.35 and 0.65 bar, while CO_2 headspace partial pressures were: 0, 0.04, 0.3 and 0.5 bar. Both H_2 and CO_2 were monitored in the gas and liquid phases by MIMS. Gas samples were taken when both MIMS signals were stable. Liquid and gas phase concentrations were analysed as detailed below. Pure ethanol was injected in the liquid phase reaching 0, 5, 10 and 30 mM. Ethanol was analysed only in the liquid phase. The data was analysed to develop a correlation with their respective MIMS signal.

2.3.2. In-process off-line data acquisition

Off-line data acquisition was performed concurrent to both batch and continuous fermentations. Samples were taken from gas and liquid phases at different times, resulting in off-line data sets, and analysed to develop a correlation with their respective MIMS signal.

2.3.3. Correlation analysis

It consisted in a linear correlation of targeted compound composition (bar or mM) vs. its respective MIMS signal magnitude (faraday).

2.3.4. In-process calibration

It consisted in splitting randomly each fermentation off-line data set into calibration and validation sets. Calibration was performed, as a linear correlation explained above, for the calibration data set.

2.3.5. Validation of MIMS calibration

It was calculated as the difference between the standard or in-process calibrated MIMS signal and its respective validation off-line data set. This difference was expressed as percentage.

2.4. Analytical methods

2.4.1. Gas phase

Gas samples of 0.5 mL were taken with a glass syringe, and analysed immediately by gas chromatography. H_2 was analysed using a GC-8A gas chromatograph (GC) equipped with a thermal conductivity detector (Shimadzu) with N_2 as a carrier gas at 100 kPa, 110 °C for the injection and detector temperature and 40 °C for the column temperature with a thermal conductivity detection (TCD) current of 80 mA. CO_2 was analysed using the same GC and conditions mentioned above, but using He as carrier gas and a current of 160 mA. Calibration was performed prior to each day's measurement using external gases provided by BOC Gases Australia Ltd. 5% CO_2 and 5% N_2 in methane, 20% CO_2 and 20% N_2 in methane, and 100% H_2, injected as 0.5 mL at 1 atm.

2.4.2. Liquid phase

Liquid samples were taken from the liquid sampling port (Fig. 1). Each liquid sample consisted of 12 mL. Two samples of 4 mL each were injected via a sterile 0.22 μm cellulose acetate cartridge into 10 mL vacuum tubes (BD Vacutainer ® serum tubes), while the

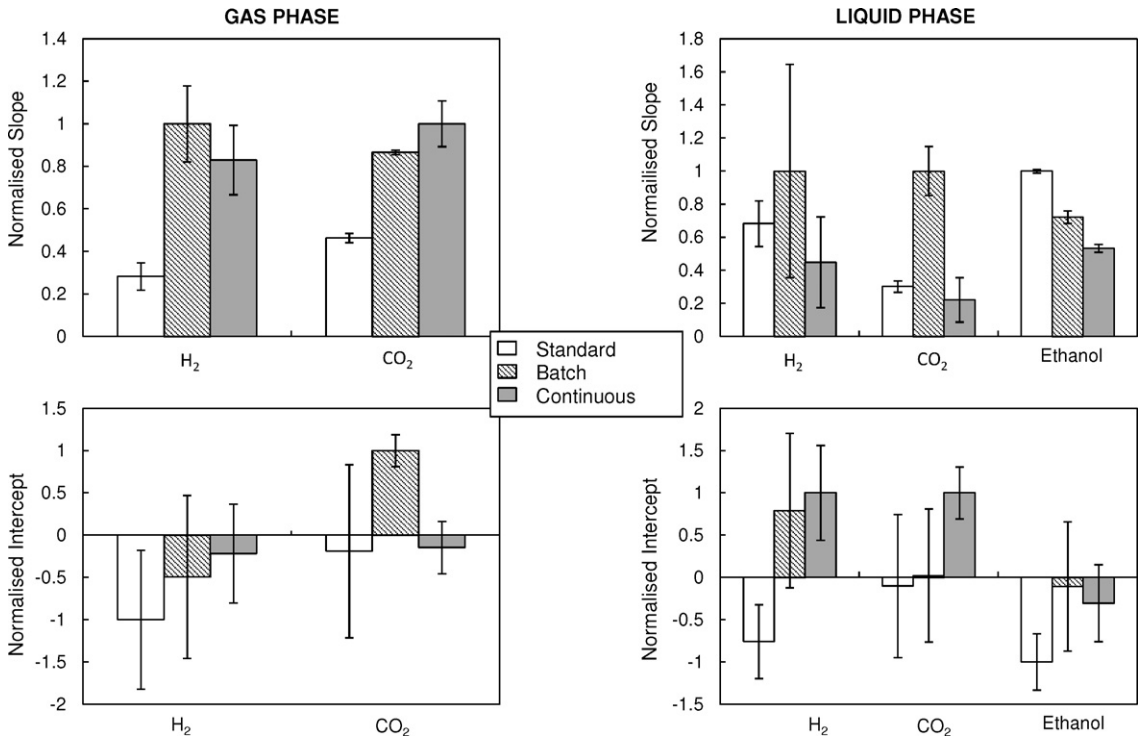

Fig. 2. Correlation analysis between MIMS signals and H_2, CO_2, ethanol concentrations. Upper charts show normalised slopes for each targeted compound at standard, batch and continuous experiments, while lower charts depict normalised intercepts. Error bars are 95% confidence with appropriate *t*-values based on degrees of freedom.

remaining 4 mL was preserved with formic acid for ethanol analysis. The tubes for dissolved CO_2 measurement were previously injected with 0.5 mL of 2 M HCl.

Dissolved gas measurement was based on an equilibrium assumption. Tubes were equilibrated for 24 h at 20 °C. 0.5 mL gas sample from each tube was measured by gas chromatography. Dissolved H_2 was measured using a GC-8 equipped with a thermal conductivity detector (Shimadzu) and a 183 cm × 0.32 cm × 26 cm stainless steel molecular sieve (80/100 mesh, washed) column. The GC was fitted with a Clarity Lite Data analysis software package. A reference and a measurement channel were used simultaneously. Those channels worked a 300 and 400 kPa, respectively using Ar as a carrier gas. Injection and detector temperatures were 80 °C and 120 °C for the column, with a TCD current of 70 mA. Calibration was performed prior to each day's measurement using external gas standards obtained from BOC Gases Australia Ltd. with concentrations in % of 0.1, 1 and 3 H_2 in N_2. Dissolved CO_2 samples were analysed as for gas phase samples.

Liquid phase H_2 or CO_2 was estimated using the temperature corrected Henry's law coefficient, and the total H_2 or CO_2 concentration in the liquid sample calculated by a mass balance. Sample liquid and gas volumes were checked by weighing on a balance.

Reactor's dissolved CO_2 concentration was then calculated as a fraction of the total CO_2 measured by this method, function of the carbonates (HCO_3^- and CO_3^{2-}) equilibrium constants and reactor's pH as is expressed in the equation below.

$$CO_{2(\text{dissolved})} = CO_{2(\text{total})} \times \frac{[H^+]^2}{[H^+]^2 + K_{a_1}[H^+] + K_{a_1}K_{a_2}}$$

Ethanol samples were preserved in 1% formic acid, and measured on a GC equipped with a polar capillary column (Agilent technologies) and a flame ionization detector (FID).

3. Results

3.1. Correlation between MIMS signals and measurement

Fig. 2 illustrates normalised slopes and intercepts for standard, batch and continuous linear correlation between MIMS signals and concentration of targeted compounds. Normalisation was based on the maximum absolute slope and intercept values found among the standard, batch and continuous correlations of each compound at liquid or gas phase.

The calculated linear correlation parameters are summarised in Table 1, where slopes and intercepts are expressed in bar·faraday^{-1} and bar for the gas phase and in mM·faraday^{-1} and mM for the liquid phase.

Errors are shown as 95% confidence in parameters, with appropriate *t*-values applied based on the number of degrees of freedom. High uncertainty in in-process correlation parameters is generally caused by a limited range in value variation as further addressed in the discussion. Similarities and differences are summarised as follow.

In the gas phase (H_2, CO_2), standard correlation slopes were consistently lower than in-process correlation slopes, indicating high sensitivity for standard conditions (see Section 4). As slopes are expressed in bar·faraday^{-1}, a given partial pressure change will produce larger MIMS signal changes in standard conditions compared to fermentation environments. Intercepts for both gases were statistically zero, except for batch CO_2 which were very low.

In the liquid phase, dissolved H_2 slopes were similar, with a mean of 9×10^5 mM·faraday^{-1}, due to the high errors. Intercept for standard correlation was the lowest, while batch and continuous intercepts were statistically the same.

Dissolved CO_2 slope for batch correlation was the highest, while standard and continuous slopes were statistically the same. Intercepts were statistically zero for standard and batch correlations while for continuous were the highest.

Table 1
Calculated linear correlation parameters between MIMS signals and H_2, CO_2, ethanol, for standard, batch and continuous experiments, with a confidence range of 95%.

	Gas phase slopes (bar·faraday^{-1})		Liquid phase slopes (mM·faraday^{-1})		
	$H_2 \times 10^{-6}$	$CO_2 \times 10^{-5}$	$H_2 \times 10^{-5}$	$CO_2 \times 10^{-7}$	Ethanol $\times 10^{-9}$
Standard	0.9 ± 0.2	3.2 ± 0.2	8 ± 2	1 ± 0.1	10 ± 1
Batch	3.2 ± 0.6	6 ± 0.07	12 ± 8	3.4 ± 0.5	7 ± 4
Continuous	2.8 ± 0.6	7 ± 0.7	6 ± 4	0.8 ± 0.5	5 ± 1.5
	Gas phase intercept (bar)		Liquid phase intercept (mM)		
	H_2	CO_2	H_2	CO_2	Ethanol
Standard	−0.13 ± 0.11	−0.002 ± 0.013	−0.14 ± 0.08	−0.1 ± 0.8	−7.7 ± 2.6
Batch	−0.06 ± 0.14	0.01 ± 0.002	0.14 ± 0.16	0.02 ± 0.8	−0.6 ± 6.3
Continuous	−0.07 ± 0.08	−0.002 ± 0.004	0.18 ± 0.11	0.9 ± 0.3	−2 ± 2

For ethanol in the liquid phase, slopes and intercepts were statistically the same or very similar due to in-process correlation high errors, caused by limited variation in the ethanol concentration during experiments (see Section 4).

As discussed further below, uncertainty in parameters, particularly slope, was strongly dependent on variation in the targeted compound. Where variation in value was low (e.g., ethanol and dissolved H_2 in batch and continuous), estimates of slope were particularly poor, as would be expected.

3.2. Fermentation kinetics

Batch and continuous fermentations were set up to investigate separately the effect of liquid and gas matrix dynamics on the translation of MIMS signal. Dynamics in the liquid matrix in batch fermentation were controlled by pH kinetics, while gas matrix dynamics in continuous fermentation were controlled by N_2 flushing. Both effects were analysed using off-line correlation of MIMS signals rather than calibration procedure (see Section 4).

Figs. 3 and 4 illustrate the MIMS signal translation by in-process correlation parameters, solid line, and standard calibration, dashed line, applied for batch and continuous fermentations, respectively. Experimental off-line correlation data set is shown as white squares. The dynamics of pH and gas flow rates are also presented in Figs. 3F and 4F.

3.2.1. Batch fermentation

Fig. 3 illustrates the kinetics of the batch experiment where the estimation of H_2 and CO_2 was substantially improved by application of in-process correlation.

Dissolved CO_2 concentration is dependent of pH. Measurement of pH dynamics, as is shown in Fig. 3F, is crucial when the dissolved CO_2 MIMS calibration method relies on an off-line analytical method that measures total inorganic carbon.

A short period of oscillation on in-process calibrated signals is observed for all the compounds and phases (see Section 4).

3.2.2. Continuous fermentation

Translated MIMS signals for the continuous experiment are shown in Fig. 4. Dynamics were induced by flushing of the headspace, and consisted of changes in N_2 flushing rates from 0 L·d^{-1}, 2.5 L·d^{-1}, 7 L·d^{-1}, and 50 L·d^{-1} as is shown in Fig. 4F.

As in the case of batch fermentation, H_2 and CO_2 estimations were also improved by the application of in-process correlation. Response of H_2 and CO_2 in the liquid was minimal, i.e., between 0.3 and 0.5 mM for H_2 and 1.2 and 1.7 mM for CO_2 (see Fig. 4A and C), while response of H_2 and CO_2 in the gas was substantial. There was also a continuous increase in ethanol concentration over the experimental period.

The solid line discontinuity in Fig. 4 is owned to an electric shortcut experienced at day 2, which led to a stop of feeding and pH pumps, and consequently a decrease on pH. MIMS signal was lost from 2.4 to 2.6 days.

3.3. In-process MIMS signal calibration

The off-line data sets shown in Figs. 3 and 4 were randomly divided into in-process MIMS calibration and validation data set for both batch and continuous fermentations. These data sets are shown in Figs. 5 and 6. The in-process calibrated curves are shown as solid lines, calibration data sets are shown as white squares and validation data sets as black circles.

3.4. Validation of calibration strategies

Table 2 illustrates the average validation errors between calibrated MIMS signals and their respective off-line experimental validation data sets for batch and continuous fermentation. The validation results of in-process and standard calibrations are presented for both fermentations. The last line of the table presents the errors for continuous fermentation with correlation parameters obtained using batch fermentation (see Section 4).

In general, these results demonstrate that in-process calibration was the best calibration strategy. For both fermentations, in-process calibration average validation errors are in the range of 10%, while for standard calibration, they are around 100%.

Special case was found for H_2 and ethanol. Validation error for H_2 gas phase was high (8 ± 70%) at continuous fermentation due to the low H_2 partial pressure caused by the N_2 flushes, while dissolved H_2 errors for both fermentations are high (−43 ± 35% for batch and 21 ± 10% for continuous) due to low response in its concentration (between 0.3 and 0.5 mM).

Ethanol errors are in the same order of magnitude, i.e., around −20% for batch and 10% for continuous fermentation (see Section 4).

4. Discussion

4.1. Standard vs. in-process calibration

The three options for calibration were standard calibration (in a water/N_2 system), calibration by standard additions, and in-process calibration. For fermentation experiments, spiking with compounds such as H_2, CO_2, bicarbonate or ethanol can have a strong influence on the biochemical process, and it is difficult to add gases for the purposes of standard additions. Therefore, we opted for standard calibration and in-process calibration. The results, particularly those in Figs. 3 and 4 demonstrate that standard calibration, even when using exactly the same equipment is ineffective for H_2 and CO_2, and may be sub-optimal for ethanol. The process

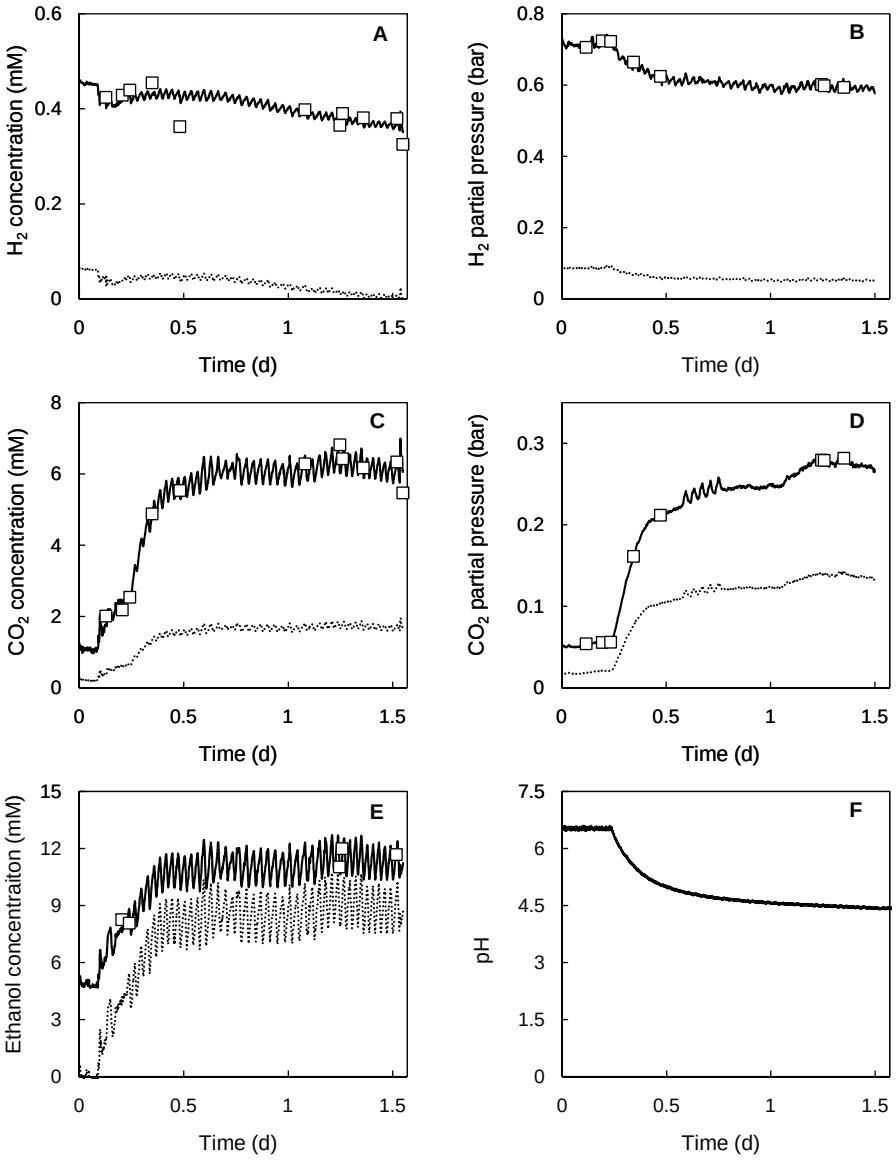

Fig. 3. MIMS signal translation of batch fermentation kinetics using batch correlation parameters, solid line, and standard calibration, dashed line. Off-line experimental data set is depicted as white squares. A and B present dissolved and gas phase H_2, C and D presents dissolved and gas phase CO_2, E shows ethanol while F presents pH kinetics.

itself has a strong impact on both measurement threshold, represented by correlation intercept, and sensitivity, represented by correlation slope. Our results confirmed that in-process calibration is necessary in fermentations to follow the evolution of analytes such as ethanol, H_2 and CO_2. In the following sections we go on to discuss how measurement of specific compounds was impacted upon by transfer issues. Compounds were divided into three classes based on liquid solubility (low/high) and volatility.

Table 2
Average validation error and its standard deviation, calculated for in-process and prior-to-fermentation-run calibration strategies.[a] Validation errors are calculated as the difference between the calibrated MIMS signal and its respective off-line experimental validation point.

	Validation errors (%)				
	Gas phase		Liquid phase		
	H_2	CO_2	H_2	CO_2	Ethanol
Batch fermentation					
In-process calibration	−3 ± 1.5	0.03 ± 3	−43 ± 35	1 ± 11	−11 ± 8
Standard calibration	−90 ± 1.5	−55 ± 7	−91 ± 5	−72 ± 3	−30 ± 14
Continuous fermentation					
In-process calibration	8 ± 70	7 ± 10	21 ± 10	3 ± 12	−3 ± 15
Standard calibration	−130 ± 40	−62 ± 10	−70 ± 20	−62 ± 5	11 ± 40
[b]Batch ferm. correlation	16 ± 60	64 ± 70	45 ± 20	50 ± 18	90 ± 35

[a] In this study it corresponds to standard calibration and continuous fermentation MIMS signal translation by batch fermentation correlation (see below).
[b] Continuous fermentation MIMS signal translation using the correlation parameters between targeted compound concentration and MIMS signal magnitudes of batch fermentation.

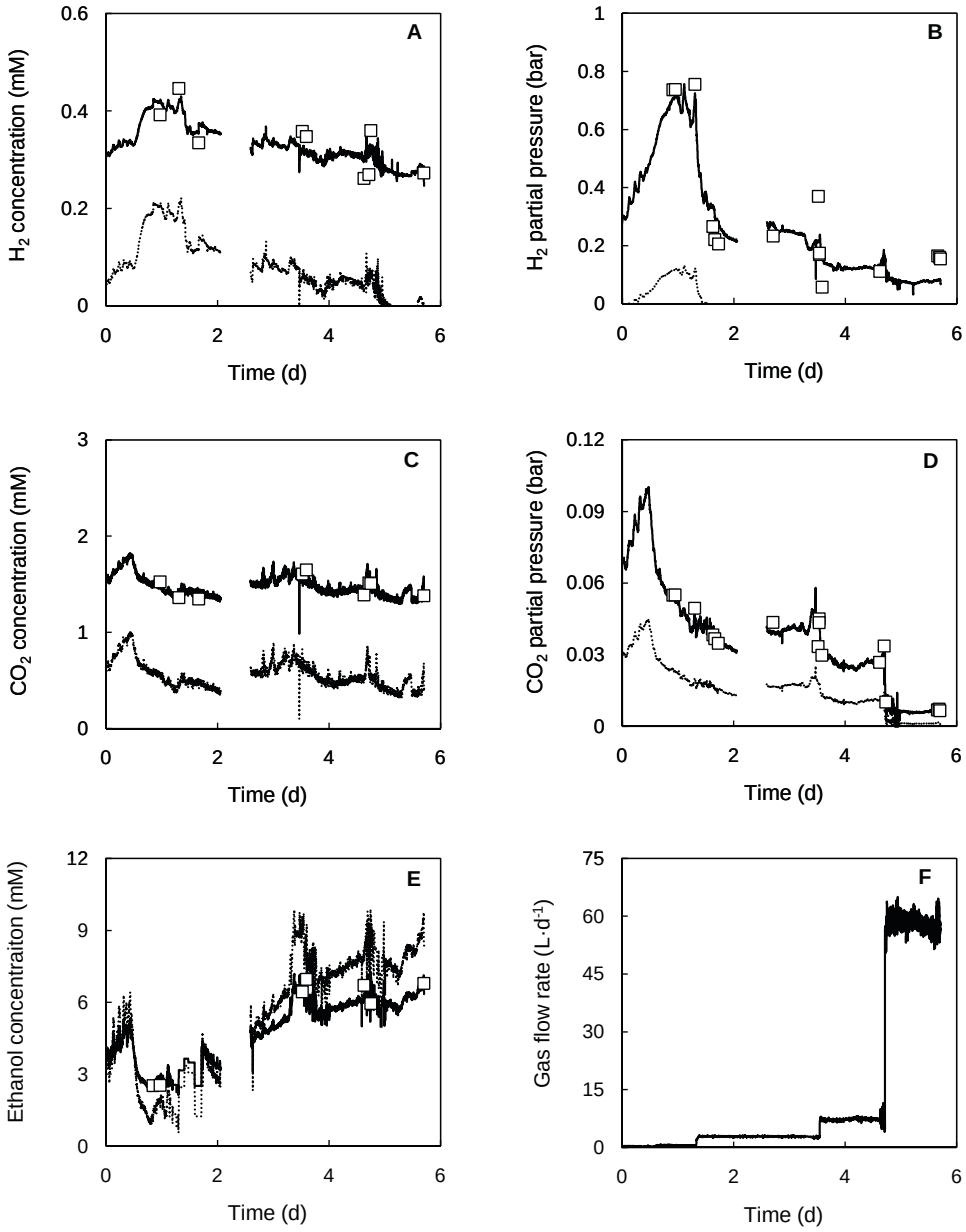

Fig. 4. MIMS signal translation of continuous fermentation kinetics by in-process continuous correlation parameters, solid line, and standard calibration, dashed line. Off-line experimental data set is depicted as white squares. The dissolved and gas phase H_2 kinetics are presented in A and B, the same is presented for CO_2 in C and D, while ethanol is shown in E and gas flow rate is presented in F.

4.1.1. Measurement in the gas phase

As is illustrated in Fig. 2 and Table 1 slope is higher for in-process calibrations, than for standard calibrations. This indicates a loss of sensitivity in the fermentation environment. By way of explanation, with standard calibrations, the headspace remains relatively dry (gas is not bubbled through the liquid). In contrast, under fermentation reactions, gas is continuously produced, which both volatilises and aspirates water. In our experiments, we noted that a liquid film formed on the surface of the MIMS probe, presenting a barrier to gas transfer. As both H_2 and CO_2 are relatively insoluble gases [25], the resistance to gas–liquid transfer is mainly in the liquid film. Such a film on the surface of the MIMS probe in a gas phase may control mass transfer, and change the characteristics completely in comparison to dry experiments, as well as make the MIMS signal strongly dependent on the thickness of the liquid film. In contrast, low variability in H_2 and CO_2 correlation intercepts (Table 1) suggests that measurement thresholds are not influenced by gas composition changes or gas turbulence caused by N_2 flushing in the continuous fermentation (Fig. 4F).

4.1.2. Detection of low solubility volatiles in the liquid phase (e.g., H_2, CO_2)

The three slopes for H_2 results presented in Fig. 2 and Table 1 appear to be similar, indicating sensitivity in the liquid phase is not particularly influenced by the matrix. Because H_2 has high diffusivity (4.65×10^{-5} cm^2·s^{-1}) [25] in pure water we expected no change in MIMS sensitivity. In contrast, intercept results suggest that a complex fermentation matrix increases the dissolved H_2 concentration threshold in fermentations compared to standard calibration (making it harder to detect). Both batch and continuous in-process calibrations correlations to be similar in terms of intercept. This can be explained according to Engel et al. [26]

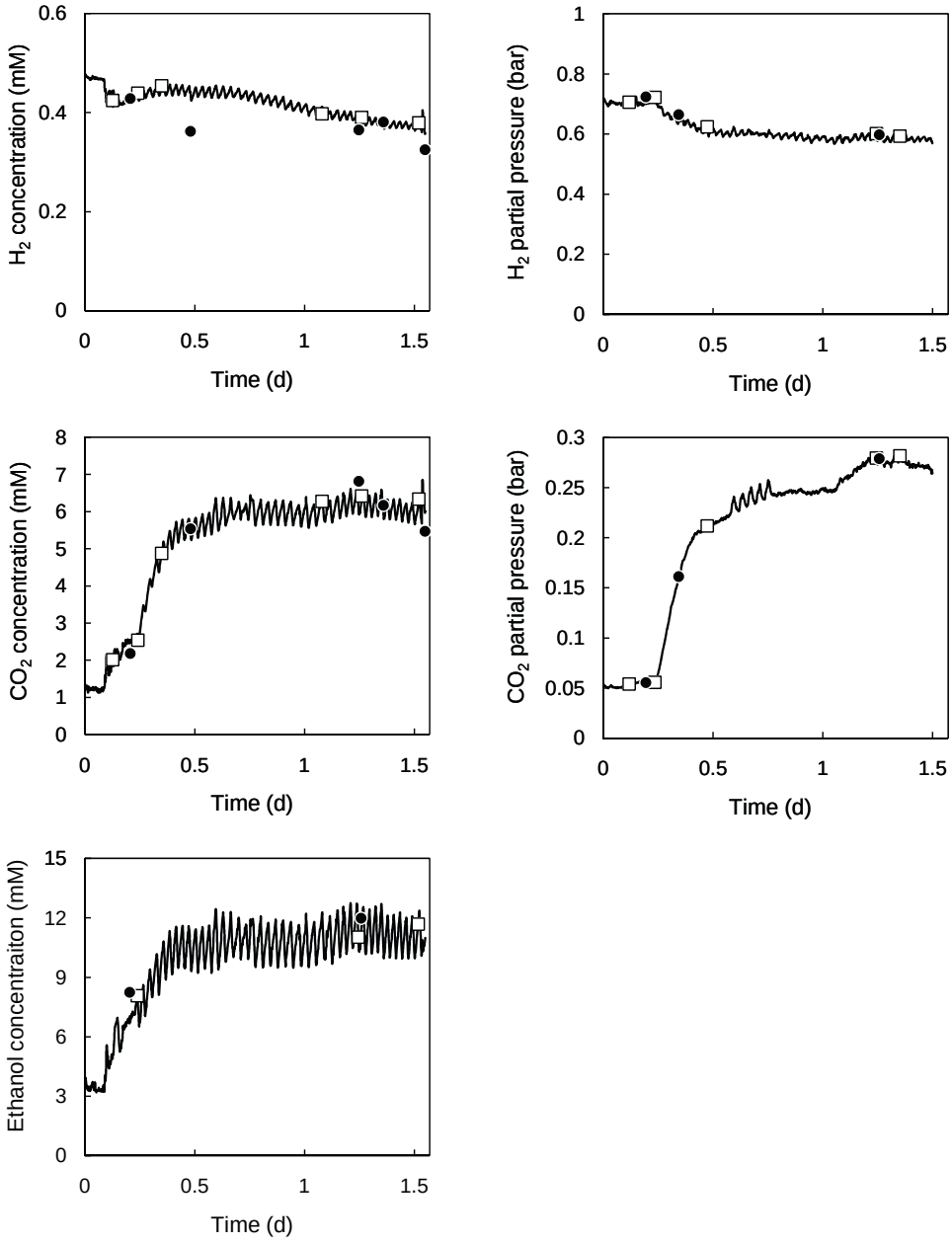

Fig. 5. Batch fermentation kinetics showing MIMS signal translation by in-process calibration, solid line, which consists in dividing the off-line experimental data set into calibration points, white squares, and validation points, black circles.

model. The average fermentation sodium bicarbonate concentration (21.5 mM) may decrease H_2 solubility by 4%, a very minor change, but possibly responsible for the change in intercept.

In the case of CO_2 the high slope at batch condition, i.e., 3.4 ± 0.5 mM·faraday^{-1} compared to approximately 1 mM·faraday^{-1} for both standard and continuous slopes, indicates a gain in sensitivity in batch fermentations. A mixed model from Schumpe et al. [27] and Gros et al. [28] indicates that non-biochemical fermentation media composition decreases CO_2 solubility by 1%, i.e., Henry constant at 36 °C (39.7 bar·L·mol^{-1}) increases to 40.2 bar·L·mol^{-1}. An alternative explanation is non-ideal solution behaviour, which would decrease the activity of the bicarbonate ion, and hence that of CO_2. This is quite likely, since at the solution ionic strength of approximately 0.2 M, the impact of ion activity is significant. However, the results show low variability in CO_2 intercept (concentration threshold), i.e., between -0.1 ± 0.8 and 0.9 ± 0.3 mM, suggesting that changes in matrix composition (the presence and changes in fermentation substrate, nutrients and products concentrations) do not affect the CO_2 concentration threshold.

4.1.3. Detection of high solubility volatiles in the liquid phase

Standard and in-process correlations for ethanol in both batch and continuous fermentations are qualitatively (Figs. 2, 3E and 4E), and statistically (Table 1) similar, but with some significant differences. Correlations between MIMS signals and ethanol concentration indicate an increase of MIMS sensitivity and concentration threshold in the fermentation matrix. Tarkiainen et al. [7] showed that sugars, salts, and CO_2 affect the MIMS response of ethanol. Glucose and sodium chloride has a positive effect, due to salting out, increasing ethanol MIMS sensitivity, while dissolved CO_2 has the opposite effect. Salts and glucose, therefore, have a higher impact in our case, even if salts were only added as necessary for biological growth. This is likely different in higher concentra-

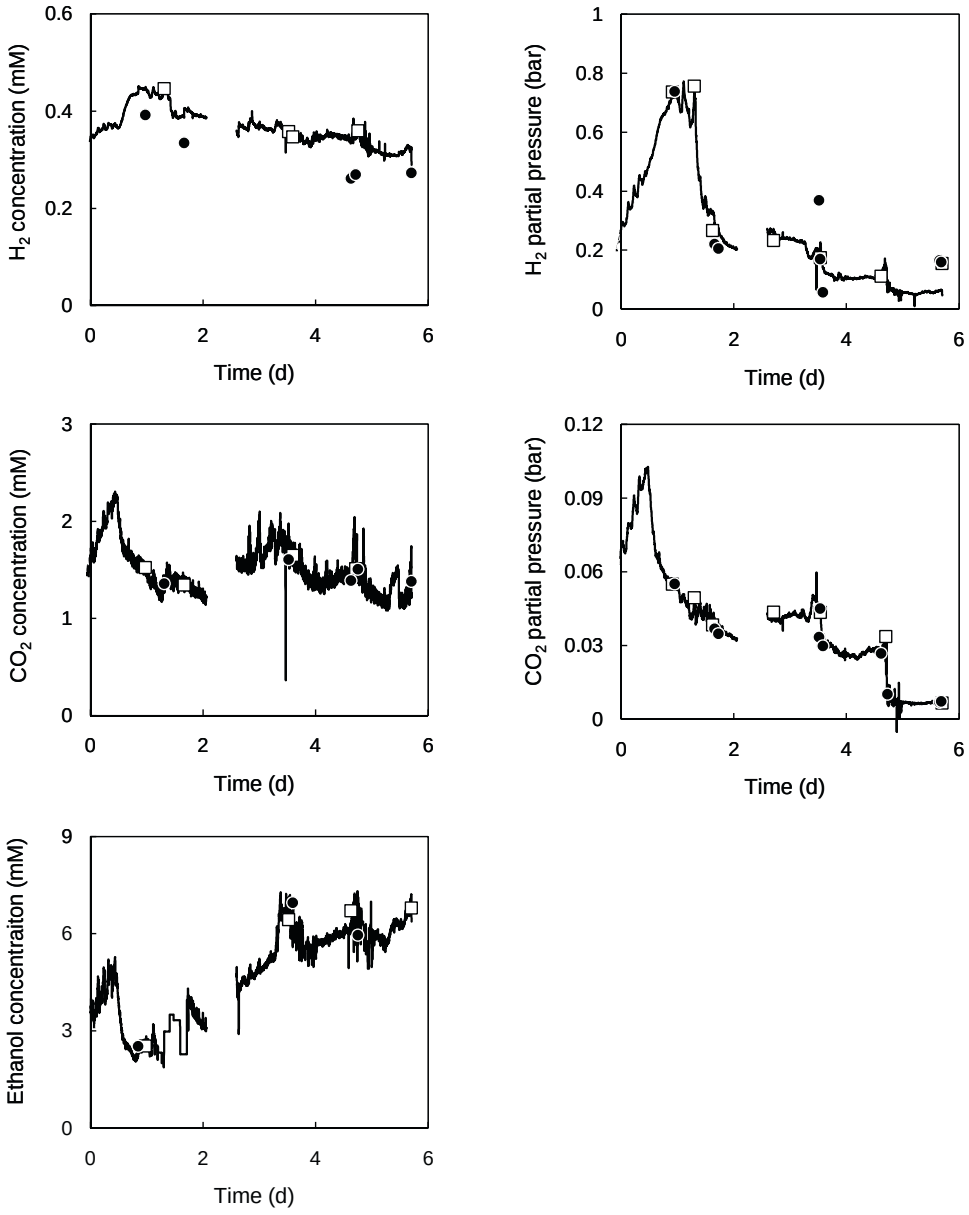

Fig. 6. Continuous fermentation kinetics showing MIMS signal translation by in-process calibration, solid line. This consists in dividing the off-line experimental data set into calibration and validation points, white squares and black circles, respectively. The lack of continuity in the solid lines was due to a shortcut.

tion waste conversion systems, where salts and ammonia have far higher concentrations. In any case, differences are low among the three correlations for ethanol H_2 and CO_2 correlations either in gas or liquid phase, as can be seen in Figs. 3 and 4.

4.2. In-process calibration

In-process calibration is necessary to calibrate fermentation MIMS signals for two reasons:

1) Each fermentation experiment is a unique and complex dynamic system that changes MIMS membrane transfer properties. Hence it is advisable to not rely on calibrations conducted prior to the experimental run. This was demonstrated for the standard calibration and even when the calibration relied on a prior fermentation as illustrated in Fig. 7. The last was also compared in terms of validation error as is presented in Table 2 where errors of this calibration strategy are largely higher than the in-process calibration.
2) In-process calibration is a relative easy and non-intrusive way to translate MIMS signals into quantifiable terms, allowing running experiments for long periods, as was the case for the continuous fermentation that lasted for 6 days.

4.3. MIMS signal oscillation and noise

Some oscillations and noise were observed in signal. Oscillations showed in Fig. 3 are due to the temperature controller (3 °C range). This temperature oscillation causes changes on diffusivity and solubility of the volatile analytes [29], which changes their flow rates through MIMS membrane and consequently their MIMS signals. These signal oscillations could be minimised using better temperature regulation, and highlight the need for good temperature control. Random noise (Fig. 4) is due to electrical issues occur-

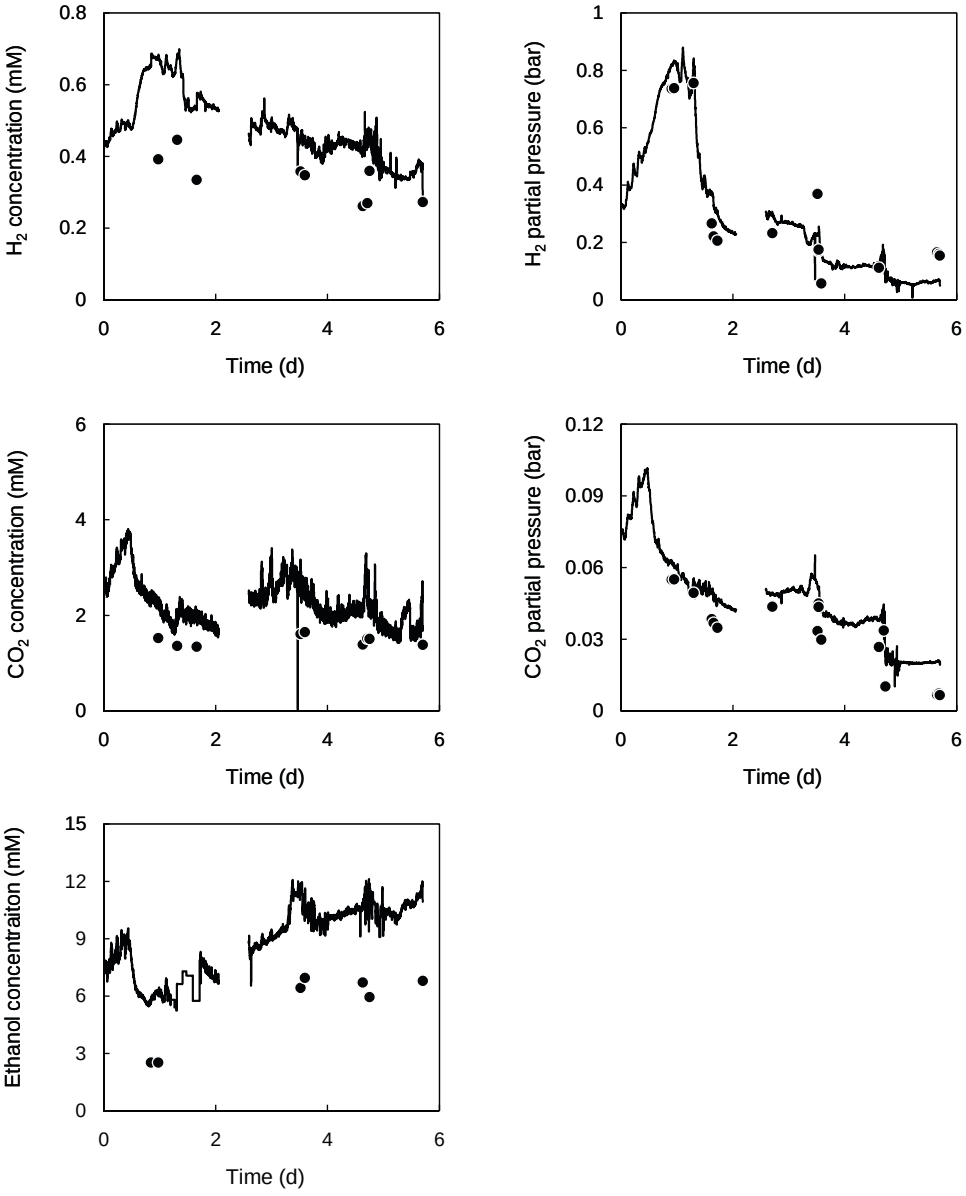

Fig. 7. Kinetics of continuous fermentation showing in solid line their respective MIMS signals translation by batch correlation parameters. Off-line validation data set is presented in black circles.

ring in the MIMS device, and can be addressed by using signal filters.

4.4. Limitations of in-process calibration

As stated above, in-process calibration is required as compared to standard or prior experiment run calibration to provide correlation between MIMS signals and actual concentrations. The main issue that we have observed is occasional low variability, which makes it very difficult to determine slope. This is especially evident in the continuous experiments (Figs. 4A, C, and E, as well as 2E). Proper determination of the calibration slope depends heavily on wide variation in concentration of the target compounds during sampling. That is, it is not useful if all samples have the same concentration. An increase of concentration variability will improve calibration, but will have an impact on the biological process. We suggest that targeted analytes be introduced at the end of the fermentation, so that concentration variability can be artificially induced increasing calibration accuracy without invalidating the experiment itself.

4.5. Applications of MIMS to fermentation experiments

Our results indicate that while standard calibration is recommended for quantifying the analyte range concentration, in-process calibration is necessary to translate signals of fermentation, which would otherwise be missed.

In fermentation processes, where dynamics play a very important role, it is very important to have a chemical analytical method with a short sample period. This is especially true for organic chemicals. Off-line analysers such as GC-FID offer non-matrix-dependant quantification, but are relatively expensive and time-consuming. With in-process calibration using MIMS, only a few off-line experimental samples are necessary to obtain an accurate view of the dynamics of the process.

An advantage of MIMS over other on-line methods is that calibration frequency is relatively long, with, in the example of Fig. 4,

six days of operation without recalibration. Other alternatives such as titrimetric off-gas analysis [30] require recalibration every 2–3 h.

The main challenge to increase the usefulness of MIMS for fermentation experiments is detection of other organic compounds such as lactic, acetic, propionic, and butyric acids. While we attempted this, detection of organic acids was not possible due to: (a) overlap in spectrum peaks, and (b) because most of these compounds have pK_a values of <5.0, and are therefore mainly present as charged (non-volatile) compounds at a pH of >5.0. The first of those 2 obstacles could be overcome by either an increase in MS accuracy (allowing for differentiation of compounds with the same MW, but different atomic formulas), and/or advanced regression techniques. The second requires accounting for both solution non-ideality, and pH, as well as possibly, off-line titration. Addressing these issues would make MIMS a requisite instrument for analysing fermentation and other mixed-culture biotechnological processes.

Acknowledgements

This research was supported under Australian Research Council's *Linkage Projects* funding scheme (project number LP0669527). J.R. Bastidas-Oyanedel acknowledges the support received by the PhD scholarship from the Chilean Commission for Science and Technology (CONICYT). Travel support was provided by the Anamix IRSES EU Project Contract Grant No. GA-2008-230829.

Authors would like to thank PhD candidate Hang Zheng (BioMass BioEnergy Group, School of Engineering, The University of Queensland) for the help measuring dissolved H_2 analysis; Dr. Oriol Gutierrez (Advance Water Management Centre, The University of Queensland) and Dr. Raymond Zeng for their pertinent commentaries and discussions.

References

[1] R. Johnson, R. Cooks, T. Allen, M. Cisper, P. Hemberger, Mass Spectrom. Rev. 19 (2000) 1–37.
[2] D. Lloyd, R. Scott, J. Microbiol. Methods 1 (1983) 313–328.
[3] R. Bell, R. Short, F. van Amerom, R. Byrne, Environ. Sci. Technol. 41 (2007) 8123–8128.
[4] T. Yang, C. Wittman, E. Heinzle, Rapid Commun. Mass Spectrom. 17 (2003) 2721–2731.
[5] B. Ferreira, F. van Keulen, M. da Fonseca, J. Membr. Sci. 208 (2002) 49–56.
[6] E. Heinzle, R. Lafferty, Eur. J. Appl. Microbiol. Biotechnol. 11 (1980) 17–22.
[7] V. Tarkiainen, T. Kotiaho, I. Mattila, I. Virkajarvi, A. Aristidou, R. Ketola, Talanta 65 (2005) 1254–1263.
[8] M. Reuss, H. Piehl, F. Wagner, Eur. J. Appl. Microbiol. 1 (1975) 323–325.
[9] A. Poulsen, F. Lauritsen, L. Olsen, FEMS Microbiol. Lett. 236 (2004) 261–266.
[10] K. Hillman, D. Lloyd, A. Williams, Lett. Appl. Microbiol. 7 (1988) 49–53.
[11] D. Radivojevic, M. Ruitenbeek, K. Seshan, L. Lefferts, J. Catal. 257 (2008) 255–261.
[12] J. Baumgardner, J. Quinn, G. Neufeld, J. Mass Spectrom. 30 (1995) 563–571.
[13] M. Hernandez, Membrane Introduction Mass Spectrometry for the On-Line Analysis of Volatile Organic Compounds in Aqueous Solutions, The Ohio State University, 2005.
[14] E. Pungor, C. Perley, C. Cooney, J. Weaver, Biotechnol. Lett. 2 (1980) 409–414.
[15] S. Sheppard, D. Lloyd, J. Microbiol. Methods 50 (2002) 175–188.
[16] C. Tu, E. Swenson, D. Silverman, Free Radical Biol. Med. 43 (2007) 1453–1457.
[17] B. Teeter, L. Dejarme, T. Choudhury, R. Cooks, R. Kaiser, Talanta 41 (1994) 1237–1245.
[18] A. Andersen, F. Lauritsen, L. Olsen, Biotechnol. Bioeng. 92 (2005) 740–747.
[19] T. Yang, C. Wittman, E. Heinzle, Metab. Eng. 8 (2006) 417–431.
[20] D. Lloyd, C. James, FEMS Microbiol. Lett. 42 (1987) 27–31.
[21] C. de Vos Petersen, H. Beck, F. Lauritsen, Biotechnol. Bioeng. 85 (2004) 298–305.
[22] C. Guegen, P. Tortell, Mar. Chem. 108 (2008) 184–194.
[23] P. Doerner, J. Lehmann, H. Piehl, R. Megnet, Biotechnol. Lett. 4 (1982) 557–562.
[24] I. Angelidaki, W. Sanders, Rev. Environ. Sci. Biotechnol. 3 (2004) 117–129.
[25] A. Pauss, G. Andre, M. Perrier, S. Guiot, Appl. Environ. Microbiol. 56 (1990) 1636–1644.
[26] D. Engel, G. Versteeg, W. van Swaaij, J. Chem. Eng. Data 41 (1996) 546–550.
[27] A. Schumpe, G. Quicker, W. Deckwer, Adv. Biochem. Eng. Biotechnol. 24 (1982) 1–38.
[28] J. Gros, C. Dussap, M. Catte, Biotechnol. Prog. 15 (1999) 923–927.
[29] D. Lloyd, K. Thomas, G. Cowie, J. Tammam, A. Williams, J. Microbiol. Methods 48 (2002) 289–302.
[30] S. Pratt, Z. Yuan, D. Gapes, M. Dorigo, R. Zeng, J. Keller, Biotechnol. Bioeng. 81 (2003) 482–495.